IEEE Access
Multidisciplinary | Rapid Review | Open Access Journal

Received March 13, 2021, accepted April 1, 2021, date of publication April 5, 2021, date of current version April 13, 2021.

Digital Object Identifier 10.1109/ACCESS.2021.3071136

Optimized Global Maximum Power Point Tracking of Photovoltaic Systems Based on Rectangular Power Comparison

PALLAVI BHARADWAJ[1], (Member, IEEE), AND VINOD JOHN[2], (Senior Member, IEEE)
[1]Laboratory for Information and Decision Systems, Massachusetts Institute of Technology, Cambridge, MA 02139, USA
[2]Department of Electrical Engineering, Indian Institute of Science, Bengaluru 560012, India

Corresponding author: Pallavi Bharadwaj (bpallavi@mit.edu)

ABSTRACT Global maximum power point tracking (GMPPT) refers to the extraction of the maximum power from photovoltaic (PV) modules in real time under changing ambient conditions. Due to the installation of PV systems in densely built-up areas, partial shading scenarios are commonplace. Commercially established GMPPTs suffer from low tracking speeds and inefficiency. A novel GMPPT algorithm is proposed here based on the rectangular power comparison (RPC), which exploits the fundamental relationship between the shading factor, the bypass diode voltage and the global maximum power point. The entire theoretical formulation of RPC is presented systematically for the first time. This method boasts of increased conversion speeds owing to the precomputation of the module voltage versus the shading factor correlations using the regression of diode model from the experimentally obtained bypass diode characteristics. The proposed method is simple to implement with the computational complexity of order n, which represents the number of uniquely shaded PV modules in a series string. The proposed approach addresses the much-needed intersection problem between the distributed and centralized PV systems and therefore targets PV strings which are most common in residential and small to medium scale commercial PV installations world over. The proposed approach is validated with the in-house developed prototype hardware set-up and software control implementation giving a 99% tracking efficiency with a recorded tracking time of 10 ms. The experimental results show 50 times improvement in speed and 95% increase in power gain as compared to the other popular existing methods namely scanning based GMPPT and local MPPT methods respectively, with negligible computational burden and less than 0.5% added cost to the conventional PV energy conversion system.

INDEX TERMS Efficiency optimization, global maximum power point tracking, partial shading, photovoltaic module measurements, solar energy conversion.

I. INTRODUCTION

As photovoltaics are entering mainstream energy conversion, the challenges associated with this promising renewable energy resource are entering the lime light. One such challenge is the global maximum power point tracking (GMPPT) under partial shading conditions. Partial shading refers to a condition when a PV system sees non-uniform irradiance and consequently non-uniform temperature conditions, either within the module or across different modules in an electrically connected PV array [1]. Partial shading not only reduces the output of the PV systems but if long operations are continued under this condition, without bypass diode protection, it can lead to hotspot induced breakdown of systems. Use of MPPT algorithms with local tracking abilities can lead to significant reduction in power generation of the PV system [2], [3]. In the last decade, various methods have been introduced with a global maximum power tracking objective [4], but this has not achieved widespread industrial and commercial penetration so far. Major gap in research and industrial adoption is due to the instability, high tracking time, and increased oscillations during peak tracing [2], [5] of the proposed GMPPT algorithms. To overcome the existing method limitations, it is imperative to review the state-of-the-art.

There are two aspects for power optimization in PV systems. One is hardware-based approach and the second is software-based approach. In the former approach, the PV

The associate editor coordinating the review of this manuscript and approving it for publication was Haris Pervaiz.

system is optimized by choosing either a distributed power conversion stage or a centralized power converter. Several methods of distributed MPPT are utilised in [6], [7], where separate converters are proposed for each PV module. But this increases the system cost and leads to coordination-related-reliability concerns, making the overall system complex. The other extreme to the distributed MPPT is the centralized system, wherein one single inverter controls an entire array of series and parallel connected PV modules. The tracking of global maximum power in these commercial systems either relies on slow scanning based algorithms [8] or incorporates expensive irradiance and temperature sensors dispersed throughout PV array [9]. An ideal optimized hardware solution would be to have GMPPT implemented at the intersection between distributed and centralized PV systems, which is at the level of a PV string. By definition, a PV string is an electrical connection of several PV modules in series and is the most common connection of residential and small-scale commercial PV installations world-wide. Such a PV string GMPPT algorithm is proposed and implemented in the present work.

The software based PV optimization approach mainly considers power optimization of a PV string using a GMPPT algorithm, according to which a string converter is controlled. The most famous among software based GMPPT methods are scanning based methods [8], [10]–[12], which are now being adopted by the industry. Conventional MPPT algorithms such as Perturb & Observe (P&O) and Incremental Conductance (INC) still hold a major share of industrial applications. P&O is one of the most robust and popular MPPT methods. In [13], it has been improved with a variable step size and further combined with fuzzy logic controller (FLC) with direct duty ratio control on a CUK converter which gives a tracking efficiency of 98% with a convergence speed within a couple of seconds. However, this method has not been tested for partial shading scenarios. The conventional methods of INC and P&O are now being upgraded to prevent tracking of a local maximum and loss of power [14], [15]. Methods such as enhanced perturb & observe [16] and modified beta algorithm [17] fall in this category, wherein the output characteristics of PV modules are scanned periodically and the highest peak power is tracked. This approach, however, still suffers from slow speeds and high power loss [5], [18]. The next class of GMPPT methods involve artificial neural networks (ANN) [19]–[22]. Many of the bio-inspired methods such as artificial bee colony [23], particle swarm optimization (PSO) [24], [25], gray wolfe optimization [26], [27], etc. suffer from slow tracking speeds. Out of all evolution based algorithms, particle swarm optimization (PSO) is the most famous, the ability of this algorithm to result in zero steady state oscillations when combined with direct duty ratio control is explored in [28] where it has also been modified to tackle the partial shading effects and track the global maximum power. Further optimized bio-inspired algorithms [29]–[31] include improved PSO [32], chaotic flower pollination algorithm [2] and improved bat algorithm [33]. Modified butterfly optimization algorithm is one of the bio-inspired algorithms that has been hybridized with a constant impedance method to improve the response time to one second [34]. Some other methods that have been combined into hybrid algorithms are PSO along with Distributed Evaluation [5], ANN with conventional and modified P&O or INC [19], [20]. However, these methods remain highly computationally intensive [35] and the accuracy of the output depends on the learning dataset and the initial conditions [29]. Another drawback of these methods is that these algorithms require periodic tuning [9]. A detailed review of the global maximum power tracking performance of the recently introduced algorithms is summarized extensively in [9].

The third class of GMPPT algorithms are model-based, which incorporate global peak prediction based on the real time irradiance and temperature measurements, along with array modelling parameters [36]–[38]. However these methods need expensive sensors for light and temperature estimation [9]. Further modification to this method has been carried out in terms of the introduction of empirical relationships [39]. But these empirical relationships are often inaccurate under extreme ambient conditions. The last class of GMPPT includes control-based methods such as constant input power control [35], but this method suffers from power loss due to a low voltage operation when power command exceeds the instantaneous system availability. Second such method is introduced in [6] where proportional-integral (PI) controllers are used in each distributed inverter to track individual peaks of each PV module, leading to increased component count and reliability issues.

To get the reliability of centralized inverters and maximum power extraction efficiency of distributed MPPTs having one power converter per PV module, we propose a hybrid approach which incorporates merits of both methods without suffering from their limitations. The hardware chosen is a centralized-string configuration with distributed low power voltage sensing. The software in terms of control algorithm involves a novel rectangular power comparison (RPC) based GMPPT which has been generalised for simple and unique to complex and common shading scenarios. The basis of the proposed RPC approach is the evaluation of the relative powers and therefore irradiances of different modules in a PV string using the module voltage information and the string current, which are monitored for shading detection. These measured voltages further specify the shading factor by using the bypass diode characteristics regression model, which are first time applied for global maximum power point tracking.

A. MAJOR CONTRIBUTIONS OF PROPOSED RPC-GMPPT

1) Novel RPC software algorithm which connects fundamental photovoltaic module characteristics to bypass diode physics and shading factors.
2) Novel hardware implementation using distributed, cost-effective, low power consuming, differential voltage sensors connected to centralized PV string inverter.

3) This approach avoids the use of expensive pyranometers for irradiance measurement. Further, this method requires no additional current sensors other than the existing single current sensor of the centralised string inverter.
4) As this method computes only shading information from module voltages, with one-time pre-determined offline correlations, it makes the algorithm faster and computationally simple.
5) This approach can detect if one or more modules in a PV string is partially shaded or under-performing due to fault or dust deposition, thus helps in reliability studies along with partial shading detection and mitigation.
6) The proposed method tracks the global maximum power with 99% tracking efficiency with high-speed, showing a recorded tracking time within ten milliseconds.
7) As compared to the popular scanning based GMPPT methods, this proposed method is significantly faster in the order of fifty times.
8) When compared to the local maximum power point tracking (LMPPT) methods, this method tracks much higher power under partial shading conditions of the order of 95%.
9) This method can be retrofitted with existing PV strings with a very low incremental cost of less than 0.5% of system cost as quantified in Appendix B.

Organisation of the subsequent sections involve treatment of the theoretical formulation of proposed RPC-GMPPT in Section II. The challenges for GMPPT implementation and their solutions are discussed in Section III, along with the proof of concept, experimental validation and benchmarking of the proposed method. Section IV discusses further simplifications, limitations, and the way forward for this approach including open questions and Section V concludes this paper. This is followed by Appendix A which details the partial shading detection aspect of the RPC-GMPPT. The second Appendix B discusses the economic aspect of the proposed approach and Appendix C discusses the effect of changing ambient conditions on the RPC-GMPPT formulation.

II. THEORY

The information of the optimal operating point in a given PV system lies in its electrical characteristics. But scanning the complete current-voltage $I - V$ or power-voltage $P-V$ characteristics loses time and energy. This information, however, can be readily obtained by noting the bypass diode voltage, string current and the module shading information. In this section, the numerical relationship between different module shading and PV string's global maximum power is first explained, followed by the determination and use of bypass diode characteristics. Further, these bypass diode characteristics are linked with relative shading to complete the novel GMPPT algorithm.

To understand the basis of this approach, consider two PV modules connected in series. Under uniform irradiance and temperature conditions, both modules have identical electrical characteristics. PV string output in this case will have double the power due to doubling of the voltage for same current. If however partial shading occurs on this two-module PV string, then there are two power peaks as one PV module gets higher irradiance than the other. Out of these two local peaks, global peak can be determined depending on which area is larger on the current-voltage curve, depicted by A and B in Fig. 1. The PV voltage changes little with respect to the irradiance, owing to its logarithmic dependence on light [40]. But PV current witnesses a linear variation with irradiance. Therefore, if irradiance on the second PV module falls to half with respect to the first PV module, its short circuit current will also fall to half. Since the voltage at the second peak is double, the area of the two rectangles will be equal if the irradiance on second module is half that of the first module and both local peaks will be of equal power value. On same lines, when the second module irradiance is less than half of the first PV module, the rectangular area B is smaller and therefore the first peak near the short circuit is higher and vice versa. This approach is named here as the rectangular power comparison (RPC) approach, the real contribution of which is to reach GMPP without scanning the complete $I - V$ or $P - V$ characteristics.

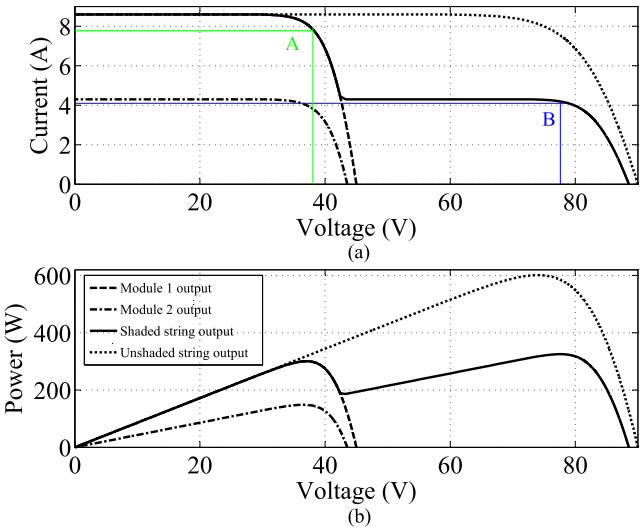

FIGURE 1. Output current-voltage (a) and power-voltage (b) characteristics of a two module PV string facing uniform and non-uniform irradiance input. Area of the rectangle A and B in (a) represents the relative powers of two peaks in (b), the higher of which is the global maximum.

To generalise this theory, consider a PV string of n PV modules connected in series, as shown in Fig. 2, where the respective module irradiances are marked as G_1 to G_n. These irradiance values can be classified in the descending order as shown in (1), without any loss of generality.

$$G_1 \geq G_2 \geq \ldots . \geq G_{n-1} \geq G_n \tag{1}$$

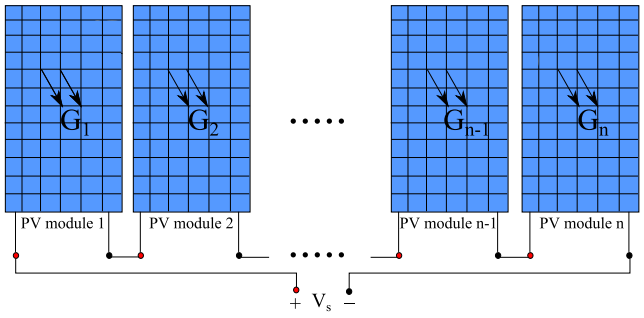

FIGURE 2. Representation of a PV string consisting of n series connected modules facing different irradiances marked as G_1 to G_n. If G_1 to G_n are equal, it results in uniform irradiance and their inequality results in the partial shading scenario.

It has been established in literature [16], that local MPPs occur at the multiples of open circuit voltage of an individual PV module scaled by a factor α, which varies from [0.8,0.9], depending on the real time ambient conditions. Therefore for a n module PV string there are n possible local peaks, out of which the global maximum needs to be identified. Mathematically, the global power optimization problem can be formulated as (2)-(3), wherein out of the n local maxima occurring each at $i\alpha V_{oc}$, i is to be found which corresponds to the global maximum.

$$V_{LMPP,\,i} = i\alpha V_{oc}, \quad i \in [1, n] \tag{2}$$

$$V_{GMPP,\,i} = Max_{V_{LMPP,\,i}}(P_{LMPP,\,i}) \tag{3}$$

For simplicity of expression, $P_{LMPP,\,i}$ is expressed as P_i in the text to follow, where i is defined as the index of the local maximum power point which varies from 1 for uniform irradiance to n for all uniquely shaded PV modules, each having a bypass diode across it.

A. SHADING FACTOR CORRELATION WITH GLOBAL MAXIMUM POWER

To solve this optimization problem, a new term called the shading factor is defined, which relates a given PV module's irradiance with respect to the most irradiated module within the PV string, which in turn is considered as the first module. Mathematically, the shading factor for the PV module i is defined in (4) as

$$K_i = \frac{G_i}{G_1} \tag{4}$$

where, irradiances G_i with index $i \in [1, n]$, are the irradiances of different modules in a n module PV string. To determine the global maximum power, consider a generalised irradiance pattern as shown in (5) for the n module PV string with $r + 1$ modules facing common irradiance.

$$G_1 > G_2 > G_3 > \ldots\ldots > G_{w-1} > G_w = G_{w+1} = \ldots \\ \ldots = G_{w+r} > G_{w+r+1} > \ldots > G_{n-1} > G_n \tag{5}$$

Current voltage characteristic of this PV string under the given irradiance pattern of (5) is shown in Fig. 3, wherein the local MPPs in terms of power P_i with voltage $V_{LMPP,i} = i\alpha V_{oc}$ and current $I_{LMPP,i} = K_i\beta I_{sc}$ are shown. Here, I_{sc} and V_{oc} are the short circuit current and open circuit voltage of the unshaded PV module in the string. Factor α determines the ratio of the maximum power point voltage to the open circuit voltage and the factor β represents the ratio of the maximum power point current to the short circuit current. These α and β parameters are fixed for a PV module under given ambient conditions and are usually in [0.8,0.9] value range [16]. Shading factor K_i holds the shading information for the i^{th} module with respect to the base module, which in turn is the most irradiated. To determine the maximum power point, the local maximum powers are compared which are given as:

$$P_i = K_i\beta I_{sc} \times i\alpha V_{oc} \tag{6}$$

It has been assumed that I_{sc} and V_{oc} for all unshaded modules under given ambient conditions remain fixed. Further, the product of α and β determines the fill factor, which does not change significantly under shading. The assumptions for this are provided in Appendix C, which shows that the small variations of the α and β parameters in time due to changing ambient conditions are addressed by the perturb and observe MPPT, which is the second layer of the proposed GMPPT method for exact peak tracking. Therefore, the initial assumptions to simplify the GMPPT problem of (3) and (6), will not affect the accuracy of the proposed algorithm.

Thus, the optimization problem of (3) and (6), can be reduced to (7), which is a simple linearly scaled comparison of shading factors. The proposed RPC based global maximum power point tracking can therefore, be mathematically formulated as:

$$Max_i(iK_i)\ where\ i \in [1, n] \tag{7}$$

Therefore, once the shading factors are known, the GMPPT problem is reduced to a n^{th} order maximum determination in a numerical vector. Since the complexity of this problem is only n, it can be easily scaled to PV strings with large number of series modules. When r modules in a PV string see equal irradiance as defined in (5), then r local maximum power points are reduced as shown in Fig. 3 and the complexity of problem is $n - r$. This is explained with a five module PV string example presented below:

1) EXAMPLE: 5 MODULE PV STRING WITH NON-UNIFORM IRRADIANCE

Given a PV string with $n = 5$ PV modules in series, with each module's irradiance input related by (8).

$$G_1 > G_2 = G_3 = G_4 > G_5 \tag{8}$$

This case has three peaks occurring at αV_{oc}, $4\alpha V_{oc}$ and $5\alpha V_{oc}$. The global maximum power depends on shading factors defined as $K_2 = K_3 = K_4 = G_4/G_1$, $K_5 = G_5/G_1$. As the number of equalities is $r = 2$, only the power levels corresponding to the $(n - r = 5 - 2 = 3)$ three voltages

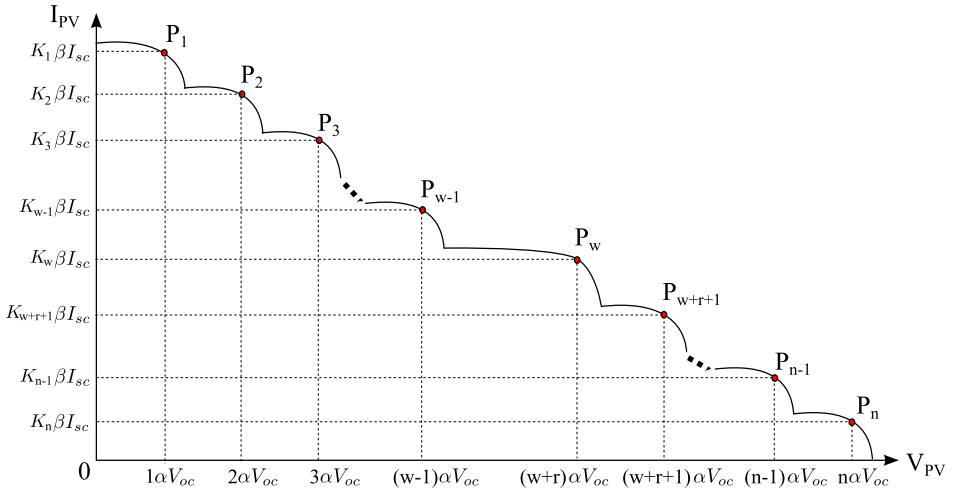

FIGURE 3. Rectangular power comparison shown on current-voltage characteristic of a n module PV string with $r+1$ modules equally irradiated and $n-r$ unequal irradiances. The global maximum power is given by the rectangle with maximum area which is determined by relative shading factors, computed through bypass diode voltage sensing.

need to be compared. From the proposed rectangular power comparison approach, the maximum value out of $1, 4K_4, 5K_5$ is to be determined. And once K_4 and K_5 are known, GMPP is also known.

2) THE CASE OF c COMMON SHADING PATTERNS

The GMPPT problem gets more and more complex when the number of shading patterns increases. However, with the help of the proposed RPC-GMPPT, this problem can be solved using the improved generalised theory for n-modules which are irradiated with G_1 to G_n irradiances with c common shading patterns as sorted in decreasing order below:

$$\begin{aligned} &G_1 > G_2 > G_3 > \ldots\ldots > G_{w_1-1} > G_{w_1} = G_{w_1+1} = \ldots \\ &\ldots = G_{w_1+r_1} > G_{w_1+r_1+1} > \ldots > G_{w_c-1} > G_{w_c} = \ldots \\ &\ldots = G_{w_c+r_c} > G_{w_c+r_c+1} > \ldots > G_{n-1} > G_n \end{aligned} \tag{9}$$

This implies that there are multiple sub-groups of PV modules which see equal irradiance within their sub-group, which is mutually exclusive with other sub-groups and other uniquely irradiated modules within the PV string. In other words, modules w_1 to $w_1 + r_1$ see one irradiance say G_{w_1}, modules w_2 to $w_2 + r_2$ see one irradiance say G_{w_2}, and so on till the c^{th} sub-group consisting of modules w_c to $w_c + r_c$ which see the irradiance G_{w_c}. Each such commonly shaded group reduces the number of local peaks by $r_j \ \forall j \in [1, c]$. In this case there are $n - \Sigma_j(r_j) \ \forall \ j \in [1, c]$ unique shading patterns and as many peak powers need to be compared. The shading factors for each group of common shading patterns is unique and its value is same for all r_j modules within each group of $j \in [1, c]$. Once the shading factors are evaluated, the global peak computation just reduces to (7) with index i defined as:

$$i = [1, w_1 - 1] \cup [w_1 + r_1, w_2 - 1] \cup \ldots \cup [w_c + r_c, n] \tag{10}$$

To determine the shading factors, the novel approach of module voltage sensing and bypass diode characterisation is used, as discussed below.

B. BYPASS DIODE CHARACTERISATION AND USE

Bypass diodes are placed in the junction box of PV modules across a certain number of PV cells in series. This ensures safe operation under shading conditions. However more often than not, the bypass diode characteristic information is not provided by the manufacturers. Therefore these characteristics are determined experimentally. To determine the bypass diode characteristic model, an experimental arrangement is made, where the PV module is kept in dark and direct current is passed through the module, till the module short circuit current and the corresponding bypass diode voltage is noted, giving an $I_{BD} - V_{BD}$ dataset. A numerical regression of this dataset into the p-n junction diode equation results in the bypass diode model as shown in Fig. 4 with an error of less than 2% under forward conduction of diode. The non-linear regression of the diode model is achieved using the Levenberg-Marquardt algorithm using MATLAB's lsqnonlin function which is programmed for non-linear least squares optimization [41]. Mathematically, the bypass diode model is represented as (11) from [42],

$$I_{BD} = I_{BDO}\left(\exp\left(\frac{V_{BD}}{m_{BD}V_T}\right) - 1\right) \tag{11}$$

where, I_{BDO} refers to the bypass diode saturation current, m_{BD} is the bypass diode ideality factor, and V_T is the thermal voltage given by $V_T = k_B T/q$, involving Boltzman's constant k_B, temperature T and the charge of an electron q. A change in irradiance does not affect the bypass diode modelling parameters directly but a change in temperature is accounted in the model by changing the thermal voltage and the saturation current, as explicitly quantified in [42]. Hence the measured

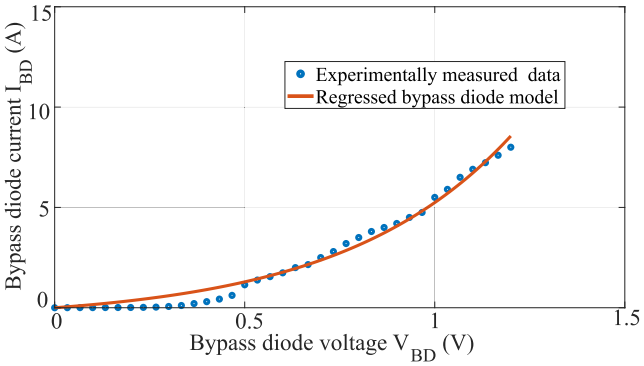

FIGURE 4. Regressed bypass diode model with experimental measurements at 25°C as reference for one bypass diode of a 300 W polycrystalline PV module.

bypass diode voltage, with known diode characteristic can be used to determine the bypass diode current under varying ambient conditions.

Once, the bypass diode is characterised, for a given bypass diode voltage V_{BD}, the bypass diode current I_{BD} is known, and the short circuit current of the shaded module i is evaluated as:

$$I_{sci} = I_{sc_1} - I_{BDi} \tag{12}$$

where, I_{sc_1} is the short circuit current of the unshaded series connected PV module or the most irradiated PV module, and is therefore equal to the string short circuit current. Therefore, a novel approach based on the PV module voltage sensing is proposed wherein experimentally modelled bypass diode characteristics are utilised for determination of the shading factor K_i.

C. DETERMINATION OF SHADING FACTOR FROM MODULE VOLTAGE

One of the major challenges in shading factor based GMPPT implementation is the determination of module irradiances. Use of irradiance sensors for each module is highly expensive and unreliable under partial shading conditions. The linear relationship between the irradiance and the short circuit current of PV module can be exploited to determine the shading factor as shown below wherein (4) can be modified to (13).

$$K_i = \frac{I_{sci}}{I_{sc1}} \tag{13}$$

Short circuit current I_{sc1} of the most irradiated PV module in a PV string is equal to the shorted string current, which is directly measured using central string inverter's current sensor. However, for the shaded PV modules the short circuit current I_{sci} measurement is evaluated using the module voltage. This novel approach prevents the introduction of additional current sensors in the circuit by using cost-effective low-power-consuming voltage sensors. The bypass diode voltage measurement is mapped into the bypass diode current using regressed diode model shown in (11). From this current, the shaded module short circuit current is calculated in (12) as the difference of the unshaded module current and the bypass diode current.

It must be noted that under uniform irradiance conditions, no PV module in a string is bypassed and all modules produce positive voltage. However, when shading occurs, the modules with low irradiance are bypassed and bypass diode enters forward conduction. Therefore the change in module voltage polarity from positive to negative is an indication of partial shading condition.

D. ALGORITHM FLOW

The complete RPC-GMPPT algorithm is summarised in Fig. 5, where the flowchart of the proposed method is presented for a generalised n-module PV string facing uniform and non-uniform irradiances. The proposed algorithm for n-module PV string considers a generalised shading pattern wherein more than one module can have equal irradiances and shading patterns as discussed in section II-A2. The steps involved in tracking the global maximum power are explained as follows:

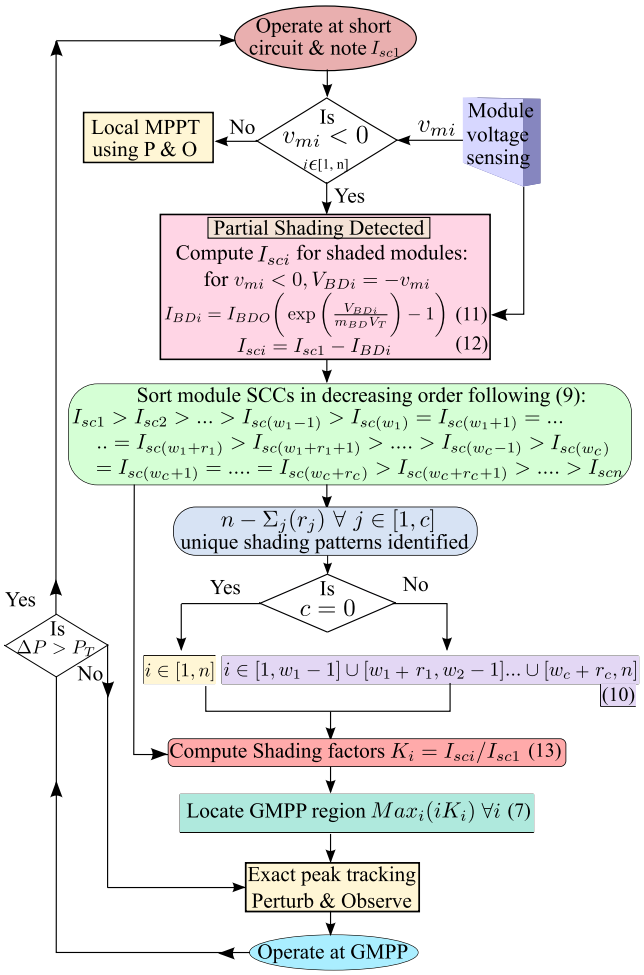

FIGURE 5. Complete RPC-global maximum power point tracking algorithm flowchart.

TABLE 1. Evaluation of GMPP with RPC for 5-module PV string under uniform and non-uniform irradiance.

Case	Module 1	Module 2	Module 3	Module 4	Module 5	$Max_i(iK_i)\forall i \in [1,5]$	V_{GMPP}
0	$K_1 = 1.0$	$K_2 = 1.0$	$K_3 = 1.0$	$K_4 = 1.0$	$K_5 = 1.0$	$Max(5 \times 1)$	$5\alpha V_{oc}$
1	$K_1 = 1.0$	$K_2 = 0.4$	$K_3 = 0.2$	$K_4 = 0.1$	$K_5 = 0.05$	$Max(1 \times 1, 2 \times 0.4, 3 \times 0.2, 4 \times 0.1, 5 \times 0.05)$	αV_{oc}
2	$K_1 = 1.0$	$K_2 = 1.0$	$K_3 = 0.7$	$K_4 = 0.42$	$K_5 = 0.21$	$Max(2 \times 1, 3 \times 0.7, 4 \times 0.42, 5 \times 0.21)$	$3\alpha V_{oc}$
3	$K_1 = 1.0$	$K_2 = 1.0$	$K_3 = 0.7$	$K_4 = 1.0$	$K_5 = 1.0$	$Max(2 \times 1, 5 \times 0.7)$	$5\alpha V_{oc}$
4	$K_1 = 1.0$	$K_2 = 0.9$	$K_3 = 0.72$	$K_4 = 0.65$	$K_5 = 0.58$	$Max(1 \times 1, 2 \times 0.9, 3 \times 0.72, 4 \times 0.65, 5 \times 0.58)$	$5\alpha V_{oc}$
5	$K_1 = 1.0$	$K_2 = 0.6$	$K_3 = 0.48$	$K_4 = 0.29$	$K_5 = 0.12$	$Max(1 \times 1, 2 \times 0.6, 3 \times 0.48, 4 \times 0.29, 5 \times 0.12)$	$3\alpha V_{oc}$

1) The individual PV module voltages are denoted by v_{mi} where $i \in [1, n]$, which are measured in real-time by voltage sensors as described in III-A.
2) Once the partial shading is detected the algorithm is triggered by operating the string at the short circuit condition and all the module voltages v_{mi} are recorded.
3) All positive v_{mi} module voltages, under short circuit condition, is an indication of uniform irradiance on the string and the local MPPT method of Perturb and Observe (P&O) is employed to detect the MPP point.
4) Negative voltage on at-least one module is an indicative of reduced irradiance or equivalently partial shading on the string. In this case, the proposed GMPPT algorithm for identifying the GMPP region is executed.
5) After the computation of the bypass diode voltage and current for the shaded modules, given by V_{BDi} and I_{BDi} respectively, short circuit currents I_{sci} are evaluated.
6) These short circuit currents (SCCs) are sorted to evaluate equal irradiance and shading patterns.
7) If common shading patterns are observed, the range of uniquely shaded module index i is modified using (10).
8) Once unique shading patterns are identified, corresponding shading factors K_i, are evaluated using (13).
9) The linearly scaled comparison based on (7) leads to the global maximum power point region occurring in one of $(i\alpha V_{oc})$ as formulated in (2)-(3).
10) To take care of small variations in α, β due to changing ambient conditions, as defined in (6), further fine-tuning to reach exact global peak power is provided with the help of P & O method.
11) The periodicity of the GMPPT algorithm is decided by observing the change in the system power above a predefined threshold, and re-initiation of the GMPPT sequence.

Change in the polarity of the individual PV module voltages is taken as an indicative of partial shading detection. The threshold value of the change in power, P_T is chosen as 5% of the initially tracked global maximum power per unit time as shown in Appendix A. This is similar to the value used in literature [12], [16], [30], and the mathematical basis behind this choice is discussed in the Appendix A for partial shading detection.

E. PROOF OF CONCEPT WITH SIMULATION RESULTS

To prove the concept behind the working of the proposed RPC-GMPPT algorithm, a 5-module 1.5 kW PV string is considered. This PV string is subjected to uniform irradiance and five kinds of different shading patterns as detailed in Table 1. These varying shading conditions include the cases of sub-groups of modules seeing common irradiance which is different than the irradiance values of other modules within the string as discussed in Section II-A2. The proposed algorithm is tested to match the results simulated from the algorithm versus the values predicted from current-voltage and power-voltage model characteristics [40] of the 5-module PV string as shown in Fig. 6. The global maximum power points as obtained from the power-voltage characteristics are seen to match the global maximum power point voltages predicted from the RPC-GMPPT as shown in Table 1, thereby proving the accuracy of the algorithm for both non-uniform, unique and common shading patterns, shown as cases 1-5 and uniform irradiance shown as case 0. To further test the algorithm, another 1.2 kW four module PV string is tested under uniform and non-uniform irradiances. Overall, seven partial shading cases along with standard test condition case of 1000 W/m^2, 25°C, called no shading case is emulated and the results obtained are shown in Fig. 7 where the identified GMPP exactly matches the GMPP estimated from the proposed RPC algorithm as detailed in Table 2. The GMPPT of a three module 0.9 kW PV string is also evaluated to prove the concept of the proposed algorithm and like earlier cases of 1.5 kW and 1.2 kW strings, the proposed algorithm passed the test with this string. The obtained global maximum power points can be seen to match the simulated power-voltage characteristics in Fig. 8 with the algorithm predicted GMPP values in Table 3.

III. EXPERIMENTAL IMPLEMENTATION

To experimentally validate this method, a buck-boost converter is connected to a rooftop PV array. The buck-boost converter is rated at 10 kW and is shown in Fig. 9. This converter is controlled using a FPGA controller. A variable resistive load of 7.5 kW is connected at the output of the buck-boost converter switching at 20 kHz. This converter can sweep the entire PV characteristics from open circuit to short circuit point and therefore can track the global maximum even under extreme shading conditions. For GMPPT determination, the module voltage sensing is required which is facilitated by the design and development of the low-cost voltage sensors. This is the subject matter of the next subsection.

A. PV MODULE VOLTAGE SENSOR

As PV modules connected in series exhibit a high common mode voltage, the designed sensor has an initial differential

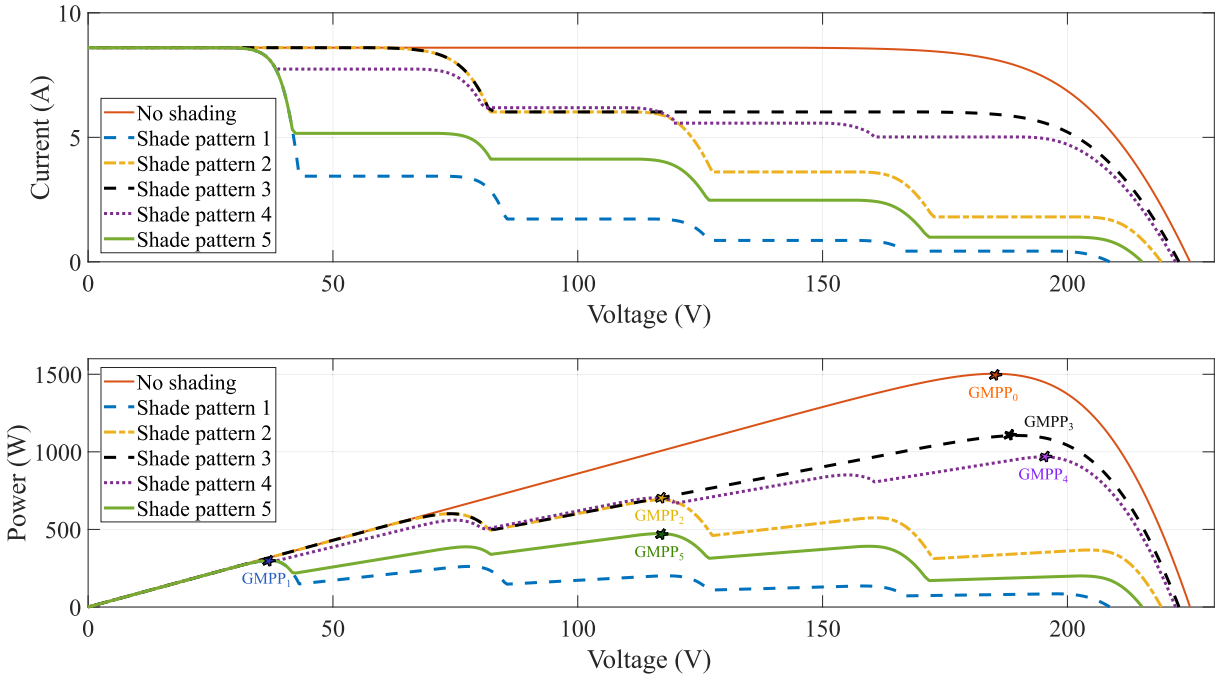

FIGURE 6. Current-voltage and power-voltage characteristics of 5-module PV string under uniform irradiance and five kinds of different shading patterns as detailed in Table 1 along with the identified global maximum power point (GMPP).

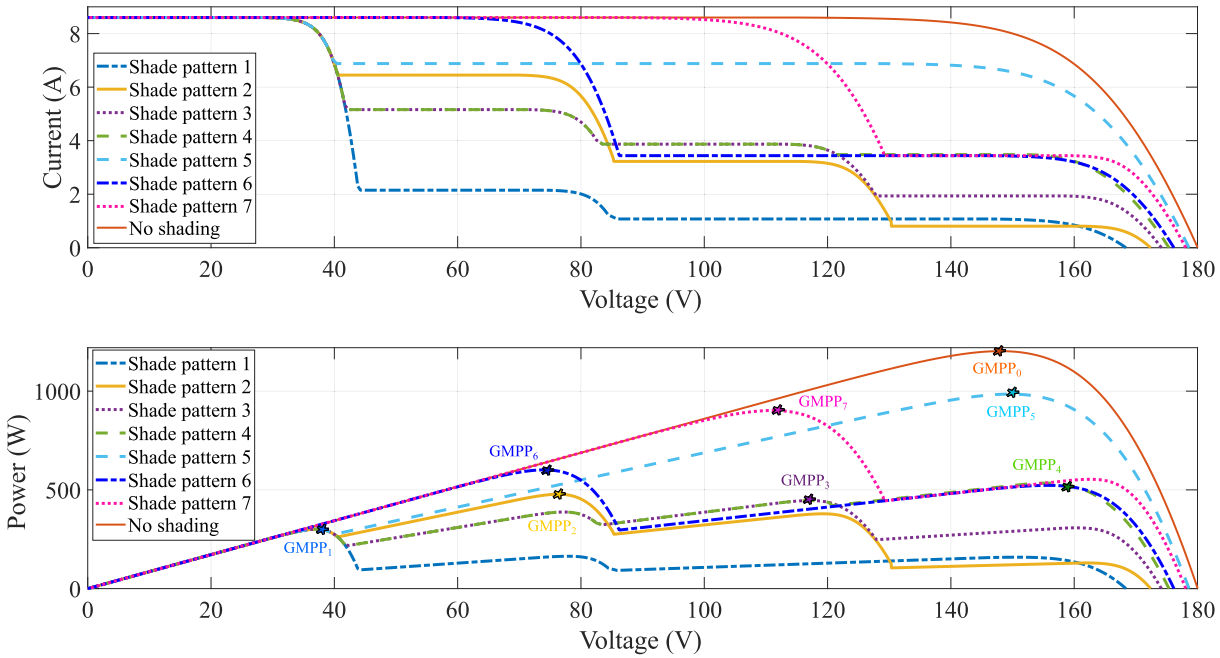

FIGURE 7. Current-voltage and power-voltage characteristics of 4-module PV string under uniform irradiance and seven kinds of different shading patterns as detailed in Table 2 along with the identified global maximum power point (GMPP).

amplifier stage. This stage has a gain of 1/3, which ensures that a single bypass diode voltage appears at the input of the second stage of the voltage amplifier, as the 300 W PV panels under study have three bypass diodes each. The second stage of this circuit is a summing amplifier with a gain such that the range for analog to digital conversion of the ADC chip in the FPGA board is not violated. Inside the FPGA controller, the proposed GMPP algorithm is coded using VHDL, which ensures that an appropriate duty ratio is given to the gate drive switching signal for the converter. The circuit schematic of the module voltage sensor is given in Fig. 10. Since the designed sensor is based on opamps, it is extremely

TABLE 2. Evaluation of GMPP with RPC for 4-module PV string under uniform and non-uniform irradiance.

Case	Module 1	Module 2	Module 3	Module 4	$Max_i(iK_i)\forall i \in [1,4]$	V_{GMPP}
0	$K_1 = 1.0$	$K_2 = 1.0$	$K_3 = 1.0$	$K_4 = 1.0$	$Max(4 \times 1)$	$4\alpha V_{oc}$
1	$K_1 = 1.0$	$K_2 = 0.25$	$K_3 = 0.12$	$K_4 = 0.12$	$Max(1 \times 1, 2 \times 0.25, 3 \times 0.12, 4 \times 0.12)$	αV_{oc}
2	$K_1 = 1.0$	$K_2 = 0.75$	$K_3 = 0.38$	$K_4 = 0.1$	$Max(1 \times 1, 2 \times 0.75, 3 \times 0.38, 4 \times 0.1)$	$2\alpha V_{oc}$
3	$K_1 = 1.0$	$K_2 = 0.6$	$K_3 = 0.45$	$K_4 = 0.22$	$Max(1 \times 1, 2 \times 0.6, 3 \times 0.45, 4 \times 0.22)$	$3\alpha V_{oc}$
4	$K_1 = 1.0$	$K_2 = 0.6$	$K_3 = 0.45$	$K_4 = 0.4$	$Max(1 \times 1, 2 \times 0.6, 3 \times 0.45, 4 \times 0.4)$	$4\alpha V_{oc}$
5	$K_1 = 1.0$	$K_2 = 0.8$	$K_3 = 0.8$	$K_4 = 0.8$	$Max(1 \times 1, 2 \times 0.8, 3 \times 0.8, 4 \times 0.8)$	$4\alpha V_{oc}$
6	$K_1 = 1.0$	$K_2 = 1$	$K_3 = 0.4$	$K_4 = 0.4$	$Max(2 \times 1, 3 \times 0.4, 4 \times 0.4)$	$2\alpha V_{oc}$
7	$K_1 = 1.0$	$K_2 = 1.0$	$K_3 = 1.0$	$K_4 = 0.4$	$Max(3 \times 1, 4 \times 0.4)$	$3\alpha V_{oc}$

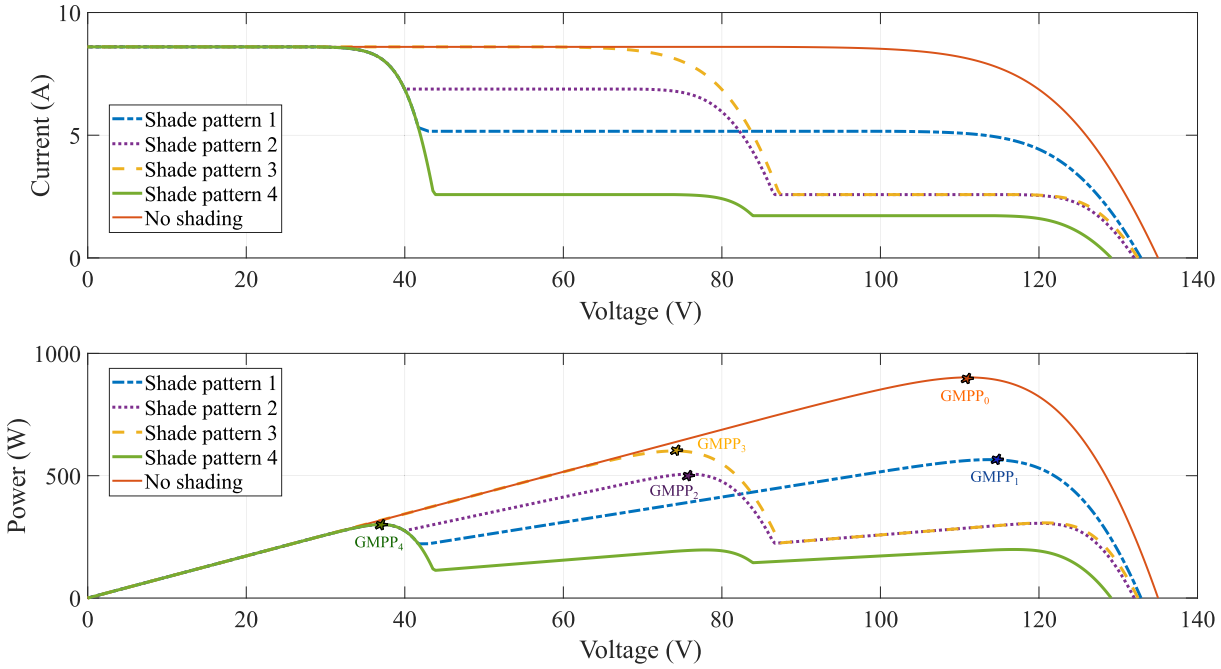

FIGURE 8. Current-voltage and power-voltage characteristics of 3-module PV string under uniform irradiance and four kinds of different shading patterns as detailed in Table 3 along with the identified global maximum power point (GMPP).

TABLE 3. Evaluation of GMPP with RPC for 3-module PV string under uniform and non-uniform irradiance.

Case	Module 1	Module 2	Module 3	$Max_i(iK_i)\forall i \in [1,3]$	V_{GMPP}
0	$K_1 = 1.0$	$K_2 = 1.0$	$K_3 = 1.0$	$Max(3 \times 1)$	$3\alpha V_{oc}$
1	$K_1 = 1.0$	$K_2 = 0.6$	$K_3 = 0.6$	$Max(1 \times 1, 2 \times 0.6, 3 \times 0.6)$	$3\alpha V_{oc}$
2	$K_1 = 1.0$	$K_2 = 0.8$	$K_3 = 0.3$	$Max(1 \times 1, 2 \times 0.8, 3 \times 0.3)$	$2\alpha V_{oc}$
3	$K_1 = 1.0$	$K_2 = 1.0$	$K_3 = 0.3$	$Max(2 \times 1, 3 \times 0.3)$	$2\alpha V_{oc}$
4	$K_1 = 1.0$	$K_2 = 0.3$	$K_3 = 0.2$	$Max(1 \times 1, 2 \times 0.3, 3 \times 0.2)$	αV_{oc}

cost and size effective. Also, the gains are chosen such that, given a sensed value of the bypass diode voltage, direct duty ratio command is given to the buck-boost dc-dc converter for global peak tracking.

B. ALGORITHM IMPLEMENTATION

The proposed RPC-GMPPT algorithm is tested for the hardware proof of concept by connecting a 0.6 kW PV string of two modules, which are unequally irradiated with shading provided using translucent shades. One 300 W PV module is unshaded and the other is horizontally shaded as shown in Fig. 11(b), such that all the substrings within the shaded panel undergo equal irradiance. The correlation between the shading factor, the bypass diode voltage, the voltage sensor output V_S and the global peak is given in Table 4 for a 2-module 600 W PV string. The determination of the shading factor K_2 from the module irradiances G_1, G_2, which are directly proportional to the module short circuit currents I_{sc1}, I_{sc2}, and its relation to the bypass diode voltage V_{BD} and current I_{BD}, for varying irradiances of the shaded module, is highlighted in this table along with the peak power (GMPP) at A (αV_{oc}) or B ($2\alpha V_{oc}$) and the corresponding duty ratio d_{GMPP} of the buck boost converter at the global maximum operating point. The PV array used for this study is shown in Fig. 11(a).

C. EXPERIMENTAL RESULTS

To validate the proposed GMPPT method, experiments are conducted under varying shading conditions and some of the results are shown in Fig. 12. The transition from one peak at

TABLE 4. Global maximum power point tracking implementation using module voltage sensing.

G_1 (W/m^2)	G_2 (W/m^2)	I_{sc1} (A)	V_S (V)	V_{BD} (V)	I_{BD} (A)	I_{sc2} (A)	K_2 -	GMPP -	d_{GMPP} -
1000	100	8.60	6.9	1.16	7.74	0.86	0.1	A at (αV_{oc})	0.65
1000	200	8.60	6.1	1.11	6.88	1.72	0.2	A at (αV_{oc})	0.65
1000	300	8.60	5.6	1.06	6.02	2.58	0.3	A at (αV_{oc})	0.65
1000	400	8.60	5.0	1.00	5.16	3.44	0.4	A at (αV_{oc})	0.65
1000	500	8.60	4.2	0.92	4.30	4.30	0.5	A at (αV_{oc})	0.65
1000	600	8.60	3.3	0.83	3.44	5.16	0.6	B at $(2\alpha V_{oc})$	0.48
1000	700	8.60	2.3	0.73	2.58	6.02	0.7	B at $(2\alpha V_{oc})$	0.50
1000	800	8.60	0.9	0.59	1.72	6.88	0.8	B at $(2\alpha V_{oc})$	0.52
1000	900	8.60	0.0	0.39	0.86	7.74	0.9	B at $(2\alpha V_{oc})$	0.55
1000	1000	8.60	0.0	0.00	0.00	8.60	1.0	B at $(2\alpha V_{oc})$	0.55

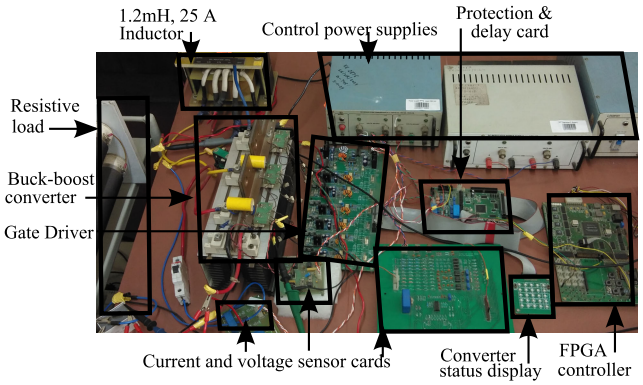

FIGURE 9. IGBT based buck boost converter along with auxiliary circuits for maximum power point tracking.

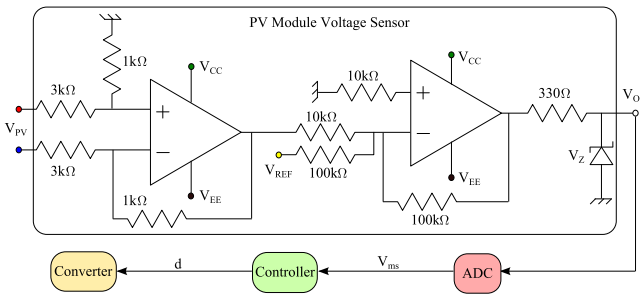

FIGURE 10. PV module voltage sensor schematic developed for partial shading detection.

B $(2\alpha V_{oc})$ to the next peak at A (αV_{oc}) is shown in Fig. 12. This transition from B to A, physically signifies the case when both PV modules in the PV string were equally shaded giving the red output characteristic in Fig. 12(a) to the condition when only the second module remains shaded, leading to the black power versus voltage characteristic in Fig. 12(a). As the controller detects a change in one of the PV module voltage polarity, it triggers the GMPPT algorithm to move from one steady state operating point shown in Fig. 12(d) to the next in Fig. 12(e). It is shown that the system takes less than 10 ms to settle at the new global maximum in Fig. 12(c).

The comparison of the proposed approach with the popular local [43] and global [17] MPPT algorithms under two very different ambient conditions is shown in Table 5. Here, the first condition marked as "peak shifting" in the table corresponds to the case of peak shifting from second peak B (at $2\alpha V_{oc}$) to first peak A (at αV_{oc}). The second condition marked as "same region" in the table corresponds to the shift in the global maximum in the same region of the second peak B (at $2\alpha V_{oc}$). It is seen that compared to scanning based s-GMPPT [17], the proposed algorithm is faster by at least 50 times, as shown in "peak shifting" and "same region" cases in the Table 5. Also, compared to the conventional P&O MPPT method [43], the proposed method improves the tracking speed by at least ten times. This is because the region of GMPPT is estimated directly from shading factor in the proposed algorithm. In terms of power capture, a major improvement of 95% is observed compared to the local MPPT [43], under shading conditions as quantified in Table 5 for the "peak shifting" case and it performs equivalent to [17], in terms of 99 % maximum power capture.

In order to analyse the obtained results, it is important to revisit the motivation of the proposed algorithm to prevent scanning of PV characteristics, which in-fact results in better speed in RPC-GMPPT. Instead of using RPC-GMPPT, if one were to scan the PV characteristic from one peak to another, then even the converter voltage and current sensors would give us the local peaks which can be compared to yield the global peak, which in-fact is done by many commercial scanning-based methods, without the module voltage sensors. The main aim of designing this smart optimized GMPPT was to prevent scanning of PV characteristics, as it has been established in literature to be time consuming and lacking in efficiency. The proposed method overcomes this limitation by one-time computation of GMPPT from looking at the module voltages at short circuit and does not need to visit all local peaks and loose time and therefore efficiency. The proposed method prevents the tedious task of scanning each peak and directly goes to the GMPP region which is fine-tuned with perturb and observe. The proposed method is much faster and more efficient than basic P&O or a scanning-based method due to the first layer of RPC-GMPPT which is built with the help of the voltage sensors and the pre-determined voltage versus shading correlations which reflect in the experimental results obtained in Table 5. The smart layer of GMPPT computation can also be achieved using a solar cell based model [40], but this requires real time computation of five

(a) (b)

FIGURE 11. (a) PV array consisting of several 300 W polycrystalline PV modules. (b) Shading arrangement used for validating the GMPPT is shown as horizontal shading.

TABLE 5. Proposed RPC-GMPPT comparison with existing methods.

Case	Tracking Time			Power Generated		
	RPC-GMPPT	s-GMPPT [17]	P&O [43]	RPC-GMPPT	s-GMPPT [17]	P&O [43]
Peak shifting	8 ms	6.0 s	0.5 s	99.0 %	90.1 %	04.0 %
Same Region	8 ms	0.5 s	0.1 s	99.0 %	99.1 %	98.0 %

modelling parameters under changing ambient conditions due to shading, which further reduces the convergence speed many-folds. This limitation is overcome by the proposed method by offline computation of bypass diode voltage versus shading correlations.

IV. DISCUSSION

Further analysis and limitations of the proposed algorithm is discussed in this section.

A. EFFECT OF SHADING ON GMPP PARAMETERS

The impact of the shading factor on the GMPP can be gauged by plotting the variation of duty ratio at the maximum power point d_{GMPP}, the maximum PV string power P_{GMPP}, the voltage at the maximum power point V_{GMPP} and the current at the maximum power point I_{GMPP} with respect to the shading factor K. A 2-module PV string is discussed here for simplicity. If one module is shaded as compared to another in an increasing fashion, the shading factor changes from 0 to 1, where 0 means full shading and 1 means both modules are equally irradiated or unshaded. Fig. 13 quantifies the effect of temperature variation on GMPP during partial shading. The simulation results, at the standard temperature of $25°C$ and at the actual experimentally measured module temperatures varying from $35 - 40°C$ during shading, show the variation in the GMPP operating point, but the same trend is followed as that for the standard temperature. It can be noticed from Fig. 13 that when shading factor is less than half, GMPP is the first peak, near the short circuit condition. Beyond 0.5 shading factor, an increase is shown for d_{GMPP}, P_{GMPP}, I_{GMPP} in Fig. 13(a), (b) and (d), but V_{GMPP} decreases linearly as shown in Fig. 13(c). Duty ratio increases and voltage decreases as GMPP shifts from open circuit to short circuit while current and power increase when second module starts seeing more light, as the shading factor increases from 0.5 to 1. This pattern further reflects that for $0 \leq K \leq 0.5$, the second PV module is bypassed and therefore has no effect on the global maximum. Thus below a shading factor of 0.5, the local MPPT can be used, as the duty ratio of the converter corresponding to the global maximum power point remains the same. This is due to the unchanging initial estimate of the converter duty ratio from the proposed GMPPT, with respect to the shading factor K, as reflected in the results of Table 4. Therefore, if the one out of two modules is shaded by more than 50%, there is no need to compute the GMPP as it will always be near the first peak corresponding to αV_{oc}, thereby further reducing the computational burden of the proposed method.

B. LIMITATIONS AND OPEN QUESTIONS

Some of the open questions that evolve from the limitations of the present method are discussed in this section. First question is the optimization of the voltage sensing mechanism. For the proof of concept, the laboratory prototype involved wired voltage sensors coupled to the PV junction connections. This works for a small PV string for residential and commercial applications, which is in the scope of the present work. However, in future, these voltage sensors can be made wireless and their positioning can be optimized in the PV terminal box. With advanced signal communication these wireless voltage sensors can talk to the smart power converters for performance optimization.

Second open question is the trade-off between the health of the PV string versus the GMPP accuracy. If the PV characteristics are continuously scanned to trace the GMPP, like many commercial systems, it may lead to accurate GMPP but due to increased losses it may severely affect the health of the PV string. This problem is solved in part by just briefly sampling the module voltages at the short circuit condition, which in the present buck-boost converter with limited current PV source is not a problem. However, in existing systems, every time shading is detected the GMPPT is triggered, which like

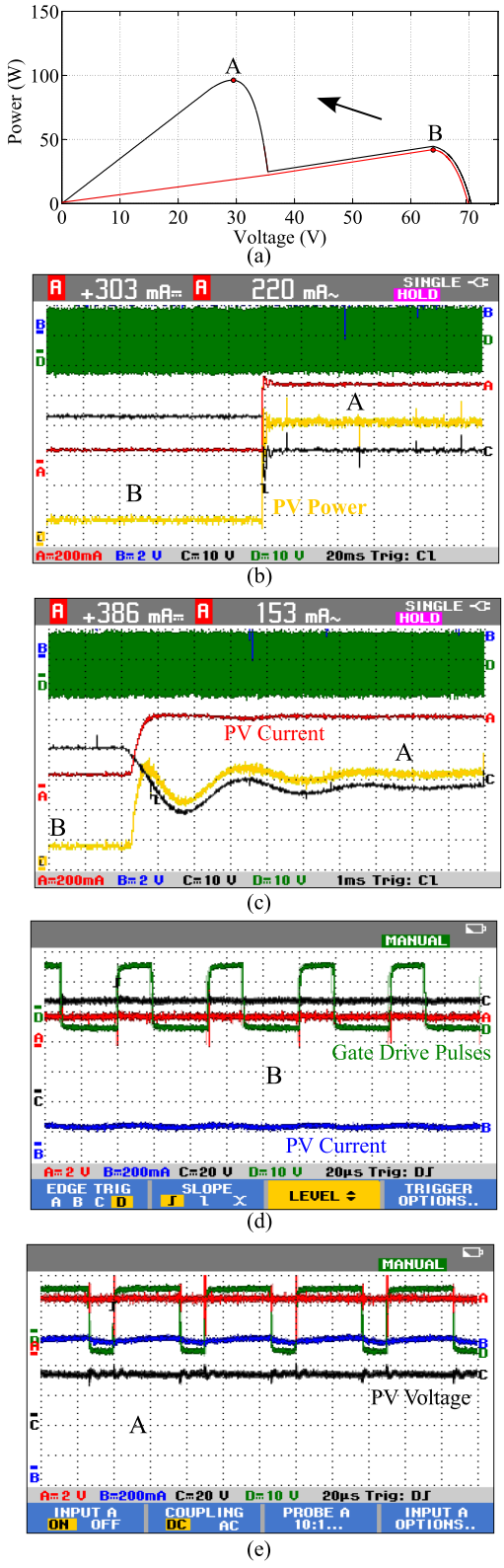

FIGURE 12. Experimental results are shown for peak B to peak A transition with the shading change as shown in (a). PV power (yellow), voltage (black), current (red) transition along with gate drive pulses (green) are shown in (b). An expanded transition with shorter time-scale is shown in (c) where the system settles in eight milliseconds. Steady state operation for state B and A are shown in (d) and (e), respectively.

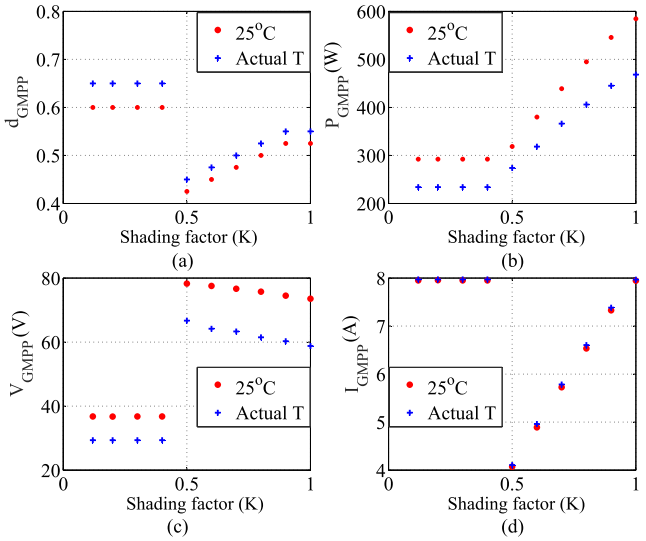

FIGURE 13. Variation of global maximum power operating point in terms of: (a) duty ratio, (b) PV power (c) PV voltage and (d) PV current with shading factor. Actual temperature marked in the figure is in the range of $35 - 40^0C$.

several popular GMPPT methods [16], relies on the threshold value of the rate of power change P_T, as in the proposed RPC-GMPPT. If P_T is too large, global maximum power will not be tracked with small changes in shading and if P_T is too small, too frequent triggering of GMPPT will affect string health. In the present method implementation, this value of P_T is taken as 5% which is 25 times higher than the quasi-static change in power due to the normal irradiance variation as established in Appendix A. This value of P_T is also seen to be in line with the value typically used in literature to trigger GMPPT in [12], [16], [30]. In future work the trade-off between the GMPPT accuracy and PV string health can be optimized for different cases, by choosing the right threshold of the GMPPT trigger parameter which further depends on how frequent and by what amount the shading patterns change for the system under consideration.

V. CONCLUSION

A novel global maximum power point tracking algorithm based on rectangular power comparison approach is proposed in this work which combines the advantages of centralized inverters and maximum power extraction efficiency of distributed MPPTs by incorporating the hybrid approach of distributed sensing and centralised power processing. The hardware chosen is a centralized-string inverter with distributed low power voltage sensing. The software in terms of control algorithm involves a novel rectangular power comparison (RPC) based GMPPT. This method incorporates bypass diode characteristics to determine the shading factor which further correlates with the global maximum for PV power output. As this method uses cost and size effective voltage sensors alone for shading determination and global maximum power tracking, it can be easily used to enhance the

existing PV systems with less than 0.5% incremental system cost. Also, the method has enhanced efficiency as it does not require time-based scanning and incorporates change in PV string power and module voltages as shading indicators. A major part of the computation is done offline in terms of the determination of the bypass diode voltage, shading factor, and global peak correlations, making the proposed method much faster and efficient. The complexity of the algorithm is of order n, representing the unique irradiance patterns and is therefore scalable to PV strings with large number of PV modules also. It is experimentally verified that the proposed method settles to the global maximum power with 99% accuracy with a tracking time of 10 ms, making it fifty times faster than the scanning based GMPPT methods and improves the power capture many-folds as compared to the local MPPT methods under partial shading conditions. The proposed PV optimization algorithm is generalised for simple and unique shading patterns to common and complex shading patterns using the systematic theoretical formulation of RPC-GMPPT algorithm. It is validated with extensive simulation and experimental results, showing improved performance over popular existing methods under varying conditions of uniform and non-uniform irradiation.

APPENDIX A
DETERMINATION OF PARTIAL SHADING BASED ON POWER CHANGE

The threshold value of the change in the tracked PV power P_T is determined for triggering the GMPPT algorithm in the flowchart shown in Fig. 5. To evaluate P_T, it is important to evaluate the steady state variation of irradiance in time. It is known that the solar irradiance G, changes with the angle of incidence θ, when measured perpendicular to the surface of the PV module, as a cosine function, represented as $G = G_o \cos\theta$, where G_o is the maximum incident irradiance. This is shown in Fig. 14. The slope of this irradiance essentially signifies the irradiance variation with the incidence angle.

$$\frac{dG}{d\theta} = G_o \frac{d\cos\theta}{d\theta} = G_o \sin\theta \tag{14}$$

The maximum value of this slope is at 90^o. To further evaluate the variation of irradiance with time, the relationship between the incidence angle and the time of the day is used. The time of day from 12 noon to 6:00 pm, marks the $0 - 90^o$ variation in the incidence angle.

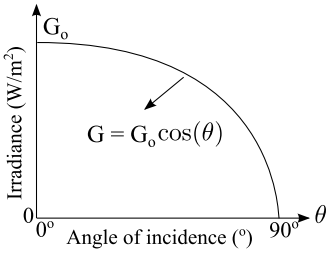

FIGURE 14. Variation of irradiance with angle of incidence measured perpendicular to the PV module surface.

$$\frac{dG}{dt} = \frac{dG}{d\theta} \times \frac{d\theta}{dt} \tag{15}$$

The maximum value of (15) is evaluated to be 4.2 $W/m^2/s$ at STC, defined as 1000 W/m^2 irradiance and $25°C$ temperature, by substituting 90^o angle of incidence. To further evaluate the effect of the change in the PV module input irradiance on its output power, the power versus irradiance relation can be derived as in (17), where the parameters are available from the PV module datasheet.

$$\left.\frac{\partial P}{\partial G}\right|_{ss} = \frac{2V_{ss}\frac{I_{L_{STC}} + K_{I_{sc}}(T_{ss} - T_{STC})}{G_{STC}}}{1 + \frac{R_s + R_{eq}}{R_{sh}} + I_{s_{ss}}\frac{R_s + R_{eq}}{mn_s V_{T_{ss}}} exp\left(\frac{V_{ss} + I_{ss}R_s}{mn_s V_{T_{ss}}}\right)} \tag{16}$$

$$\frac{dP}{dt} = \left.\frac{\partial P}{\partial G}\right|_{ss} \times \frac{dG}{dt} \tag{17}$$

From (17), the change in power with time can be estimated using (14) to (17). The subscript ss in (17) represents the initial steady state condition at which the change in power is computed, while subscript STC represents the standard test conditions of $G_{STC} = 1000\ W/m^2$ irradiance and $T_{STC} = 25°C$ temperature. The PV modelling parameters namely: the light induced current I_L, the diode dark saturation current I_s, the diode ideality factor m, the series resistance R_s, the shunt resistance R_{sh}, the temperature coefficient of short circuit current $K_{I_{sc}}$ and the number of series cells in a PV panel n_s; can be derived from the PV panel datasheet provided by the manufacturer. The real time PV terminal voltage V_{ss}, current I_{ss}, irradiance G_{ss} and temperature T_{ss} are measured at the steady state operating point. R_{eq} represents the equivalent load across the PV terminals. Substituting these values in (17) gives the variation of power with irradiance at different operating points. Based on the above relationship in (17), it is seen that an average change of 10% in light causes a 5 % change in the polycrystalline PV module power output. Since, percentage steady state irradiance variation with respect to standard irradiance of 1000 W/m^2 is computed to be $\frac{4.2\ W/m^2/s}{1000\ W/m^2} \times 100\% = 0.42\ \%/s$ in (15), its substitution in (17) leads to the maximum change of 0.21 %/s in power with time. Assuming maximum power point operation, when a power change of the order of 5 %/s and above is observed, it can be attributed to shading, because it is more than twenty times the maximum steady state variation of power with time due to normal sunlight variation in a day. Based on this mathematical background, the threshold value of change of power in time, with respect to the steady state conditions is called $P_T = 5\%/s$, which is selected to trigger the GMPPT algorithm.

APPENDIX B
INCREMENTAL IMPLEMENTATION COST

This method adds negligible cost increment of $1 per panel in the PV string (Digikey parts [44]). This amounts to less than 0.5% of total system cost including the PV panels, buck-boost

converter and installation costs [45], yet increasing typical PV annual system energy yield many-fold, along with improving system reliability by combining voltage sensing, PV modeling and inverter control all-together.

APPENDIX C
CHANGE IN FILL FACTOR WITH AMBIENT CONDITIONS

If two PV modules are considered without mismatch, then for identical irradiance and temperature conditions, their fill factor is identical, as claimed by the manufacturer datasheet. When these modules are connected in a series combination and they operate under uniform irradiance condition, then the fill factor of the string is same as that of individual PV modules without mismatch and equals $\alpha \times \beta$ as defined in Section II-A. However, when different PV modules see different irradiance, then the situation becomes complicated. To simplify this partial shading problem, it can be handled in two parts which translates to the effect on voltage and current of two factors namely: the change in irradiance due to shading and the change in module temperature due to shading. According to (6) the maximum power point current can be defined as $K_i \beta I_{sc}$ and maximum power point voltage can be defined as $i\alpha V_{oc}$. Here I_{sc} and V_{oc} are short circuit current and open circuit voltage under uniform irradiance or without non-uniform shading. Factors α and β are the factors of MPP voltage with respect to V_{oc} and MPP current with respect to I_{sc} respectively, under uniform irradiance. The effect of shading is incorporated in (6) in the shading factor K_i which also splits the single peak into n possible peaks. It is known that shading changes irradiance which is linearly proportional to current but changes voltage only in a logarithmic manner, this causes small change in α with changing irradiance due to shade. The factors α, β change due to the change in temperature resulting from shade, this again is small compared to the change due to shaded irradiance, mainly because the temperature change due to shading is only $5 - 10°C$ as established in [46]. Therefore, in the proposed approach the small changes in $\alpha \times \beta$ are handled by the second layer of GMPPT which is perturb and observe, once the proposed GMPPT identifies the global maximum power region in a certain $i\alpha V_{oc}$ voltage range.

REFERENCES

[1] Z. Bi, J. Ma, K. Wang, K. L. Man, J. S. Smith, and Y. Yue, "Identification of partial shading conditions for photovoltaic strings," *IEEE Access*, vol. 8, pp. 75491–75502, 2020.

[2] D. Yousri, T. S. Babu, D. Allam, V. K. Ramachandaramurthy, and M. B. Etiba, "A novel chaotic flower pollination algorithm for global maximum power point tracking for photovoltaic system under partial shading conditions," *IEEE Access*, vol. 7, pp. 121432–121445, 2019.

[3] W. Li, G. Zhang, T. Pan, Z. Zhang, Y. Geng, and J. Wang, "A Lipschitz optimization-based MPPT algorithm for photovoltaic system under partial shading condition," *IEEE Access*, vol. 7, pp. 126323–126333, 2019.

[4] H. Renaudineau, F. Donatantonio, J. Fontchastagner, G. Petrone, G. Spagnuolo, J.-P. Martin, and S. Pierfederici, "A PSO-based global MPPT technique for distributed PV power generation," *IEEE Trans. Ind. Electron.*, vol. 62, no. 2, pp. 1047–1058, Feb. 2015.

[5] M. Joisher, D. Singh, S. Taheri, D. R. Espinoza-Trejo, E. Pouresmaeil, and H. Taheri, "A hybrid evolutionary-based MPPT for photovoltaic systems under partial shading conditions," *IEEE Access*, vol. 8, pp. 38481–38492, 2020.

[6] Y. Guo, H. Sun, Y. Zhang, Y. Liu, X. Li, and Y. Xue, "Duty-cycle predictive control of quasi-Z-source modular cascaded converter based photovoltaic power system," *IEEE Access*, vol. 8, pp. 172734–172746, 2020.

[7] W.-L. Chen and C.-T. Tsai, "Optimal balancing control for tracking theoretical global MPP of series PV modules subject to partial shading," *IEEE Trans. Ind. Electron.*, vol. 62, no. 8, pp. 4837–4848, Aug. 2015.

[8] L. Li, Y. Chen, H. Liu, W. Tang, M. Liu, J. Wu, and Z. Li, "A multi-producer group-search-optimization method-based maximum-power-point-tracking for uniform and partial shading condition," *IEEE Access*, vol. 8, pp. 184688–184696, 2020.

[9] S. H. Hanzaei, S. A. Gorji, and M. Ektesabi, "A scheme-based review of MPPT techniques with respect to input variables including solar irradiance and PV arrays' temperature," *IEEE Access*, vol. 8, pp. 182229–182239, 2020.

[10] A. M. S. Furtado, F. Bradaschia, M. C. Cavalcanti, and L. R. Limongi, "A reduced voltage range global maximum power point tracking algorithm for photovoltaic systems under partial shading conditions," *IEEE Trans. Ind. Electron.*, vol. 65, no. 4, pp. 3252–3262, Apr. 2018.

[11] S. Selvakumar, M. Madhusmita, C. Koodalsamy, S. P. Simon, and Y. R. Sood, "High-speed maximum power point tracking module for PV systems," *IEEE Trans. Ind. Electron.*, vol. 66, no. 2, pp. 1119–1129, Feb. 2019.

[12] A. Ramyar, H. Iman-Eini, and S. Farhangi, "Global maximum power point tracking method for photovoltaic arrays under partial shading conditions," *IEEE Trans. Ind. Electron.*, vol. 64, no. 4, pp. 2855–2864, Apr. 2017.

[13] T. Radjai, J. P. Gaubert, L. Rahmani, and S. Mekhilef, "Experimental verification of P&O MPPT algorithm with direct control based on fuzzy logic control using CUK converter," *Int. Trans. Elect. Energy Syst.*, vol. 25, no. 12, pp. 3492–3508, 2015.

[14] Y. Zhu and J. Fei, "Adaptive global fast terminal sliding mode control of grid-connected photovoltaic system using fuzzy neural network approach," *IEEE Access*, vol. 5, pp. 9476–9484, 2017.

[15] L. Xu, R. Cheng, and J. Yang, "A modified INC method for PV string under uniform irradiance and partially shaded conditions," *IEEE Access*, vol. 8, pp. 131340–131351, 2020.

[16] H. Patel and V. Agarwal, "MATLAB-based modeling to study the effects of partial shading on PV array characteristics," *IEEE Trans. Energy Convers.*, vol. 23, no. 1, pp. 302–310, Mar. 2008.

[17] X. Li, H. Wen, Y. Hu, L. Jiang, and W. Xiao, "Modified beta algorithm for GMPPT and partial shading detection in photovoltaic systems," *IEEE Trans. Power Electron.*, vol. 33, no. 3, pp. 2172–2186, Mar. 2018.

[18] K. Chen, S. Tian, Y. Cheng, and L. Bai, "An improved MPPT controller for photovoltaic system under partial shading condition," *IEEE Trans. Sustain. Energy*, vol. 5, no. 3, pp. 978–985, Jul. 2014.

[19] W. Zhang, G. Zhou, H. Ni, and Y. Sun, "A modified hybrid maximum power point tracking method for photovoltaic arrays under partially shading condition," *IEEE Access*, vol. 7, pp. 160091–160100, 2019.

[20] H. M. El-Helw, A. Magdy, and M. I. Marei, "A hybrid maximum power point tracking technique for partially shaded photovoltaic arrays," *IEEE Access*, vol. 5, pp. 11900–11908, 2017.

[21] B.-R. Peng, K.-C. Ho, and Y.-H. Liu, "A novel and fast MPPT method suitable for both fast changing and partially shaded conditions," *IEEE Trans. Ind. Electron.*, vol. 65, no. 4, pp. 3240–3251, Apr. 2018.

[22] B. N. Alajmi, K. H. Ahmed, S. J. Finney, and B. W. Williams, "A maximum power point tracking technique for partially shaded photovoltaic systems in microgrids," *IEEE Trans. Ind. Electron.*, vol. 60, no. 4, pp. 1596–1606, Apr. 2013.

[23] K. Sundareswaran, P. Sankar, P. S. R. Nayak, S. P. Simon, and S. Palani, "Enhanced energy output from a PV system under partial shaded conditions through artificial bee colony," *IEEE Trans. Sustain. Energy*, vol. 6, no. 1, pp. 198–209, Jan. 2015.

[24] S. Obukhov, A. Ibrahim, A. A. Zaki Diab, A. S. Al-Sumaiti, and R. Aboelsaud, "Optimal performance of dynamic particle swarm optimization based maximum power trackers for stand-alone PV system under partial shading conditions," *IEEE Access*, vol. 8, pp. 20770–20785, 2020.

[25] K. Ishaque and Z. Salam, "A deterministic particle swarm optimization maximum power point tracker for photovoltaic system under partial shading condition," *IEEE Trans. Ind. Electron.*, vol. 60, no. 8, pp. 3195–3206, Aug. 2013.

[26] K. Guo, L. Cui, M. Mao, L. Zhou, and Q. Zhang, "An improved gray wolf optimizer MPPT algorithm for PV system with BFBIC converter under partial shading," *IEEE Access*, vol. 8, pp. 103476–103490, 2020.
[27] S. Mohanty, B. Subudhi, and P. K. Ray, "A new MPPT design using grey wolf optimization technique for photovoltaic system under partial shading conditions," *IEEE Trans. Sustain. Energy*, vol. 7, no. 1, pp. 181–188, Jan. 2016.
[28] K. Ishaque, Z. Salam, M. Amjad, and S. Mekhilef, "An improved particle swarm optimization (PSO)–based MPPT for PV with reduced steady-state oscillation," *IEEE Trans. Power Electron.*, vol. 27, no. 8, pp. 3627–3638, Aug. 2012.
[29] H. Li, D. Yang, W. Su, J. Lu, and X. Yu, "An overall distribution particle swarm optimization MPPT algorithm for photovoltaic system under partial shading," *IEEE Trans. Ind. Electron.*, vol. 66, no. 1, pp. 265–275, Jan. 2019.
[30] Q. Zhu, X. Zhang, S. Li, C. Liu, and H. Ni, "Research and test of power-loop-based dynamic multi-peak MPPT algorithm," *IEEE Trans. Ind. Electron.*, vol. 63, no. 12, pp. 7349–7359, Dec. 2016.
[31] C. Manickam, G. R. Raman, G. P. Raman, S. I. Ganesan, and C. Nagamani, "A hybrid algorithm for tracking of GMPP based on P&O and PSO with reduced power oscillation in string inverters," *IEEE Trans. Ind. Electron.*, vol. 63, no. 10, pp. 6097–6106, Oct. 2016.
[32] K. Hu, S. Cao, W. Li, and F. Zhu, "An improved particle swarm optimization algorithm suitable for photovoltaic power tracking under partial shading conditions," *IEEE Access*, vol. 7, pp. 143217–143232, 2019.
[33] C. Y. Liao, R. K. Subroto, I. S. Millah, K. L. Lian, and W.-T. Huang, "An improved bat algorithm for more efficient and faster maximum power point tracking for a photovoltaic system under partial shading conditions," *IEEE Access*, vol. 8, pp. 96378–96390, 2020.
[34] I. Shams, S. Mekhilef, and K. S. Tey, "Maximum power point tracking using modified butterfly optimization algorithm for partial shading, uniform shading, and fast varying load conditions," *IEEE Trans. Power Electron.*, vol. 36, no. 5, pp. 5569–5581, May 2021.
[35] E. Koutroulis and F. Blaabjerg, "A new technique for tracking the global maximum power point of PV arrays operating under partial-shading conditions," *IEEE J. Photovolt.*, vol. 2, no. 2, pp. 184–190, Apr. 2012.
[36] Y. Mahmoud and E. F. El-Saadany, "Fast power-peaks estimator for partially shaded PV systems," *IEEE Trans. Energy Convers.*, vol. 31, no. 1, pp. 206–217, Mar. 2016.
[37] Y. Hu, W. Cao, J. Wu, B. Ji, and D. Holliday, "Thermography-based virtual MPPT scheme for improving PV energy efficiency under partial shading conditions," *IEEE Trans. Power Electron.*, vol. 29, no. 11, pp. 5667–5672, Nov. 2014.
[38] P. Bharadwaj and V. John, "Shading fraction based global maximum power prediction for photovoltaic energy conversion systems," in *Proc. IEEE 7th World Conf. Photovoltaic Energy Convers. (WCPEC) (Joint Conf. 45th IEEE PVSC, 28th PVSEC 34th EU PVSEC)*, Jun. 2018, pp. 1163–1168.
[39] J. Ahmed and Z. Salam, "An improved method to predict the position of maximum power point during partial shading for PV arrays," *IEEE Trans. Ind. Informat.*, vol. 11, no. 6, pp. 1378–1387, Dec. 2015.
[40] A. Chatterjee, A. Keyhani, and D. Kapoor, "Identification of photovoltaic source models," *IEEE Trans. Energy Convers.*, vol. 26, no. 3, pp. 883–889, Sep. 2011.
[41] *Lsqnonlin, MATLAB Non Linear Model Fitting*. MATLAB R2020b. Accessed: Mar. 3, 2021. [Online]. Available: https://www.mathworks.com/help/optim/ug/lsqnonlin.html
[42] M. K. Achuthan and K. N. Bhat, *Fundamentals Semiconductor Devices*. New York, NY, USA: McGraw-Hill, 2012.
[43] P. Bharadwaj and V. John, "Direct duty ratio controlled MPPT algorithm for boost converter in continuous and discontinuous modes of operation," in *Proc. IEEE 6th India Int. Conf. Power Electron. (IICPE)*, Dec. 2014, pp. 1–6.
[44] *Digikey Online Directory*. Accessed: Sep. 3, 2019. [Online]. Available: https://www.digikey.com/
[45] P. Bharadwaj and V. John, "Comparison of grid-tied and dual mode PV system considering grid outage duration," in *Proc. Indo-German Conf. Sustainability*, Feb. 2016, pp. 1–6.
[46] P. Bharadwaj and V. John, "Subcell modeling of partially shaded photovoltaic modules," *IEEE Trans. Ind. Appl.*, vol. 55, no. 3, pp. 3046–3054, May 2019.

PALLAVI BHARADWAJ (Member, IEEE) received the B.E. degree in electrical engineering from the Delhi College of Engineering, Rohini, India, in 2012, and the M.E. degree from the Indian Institute of Science, Bengaluru, India, in 2014, and the Ph.D. degree from the Department of Electrical Engineering, Indian Institute of Science, in 2019. She is currently a Postdoctoral Research Associate with the Laboratory for Information and Decision Systems, Massachusetts Institute of Technology, Cambridge, MA, USA. Her current research interests include photovoltaic power conversion, power quality for renewable energy systems, and energy optimization.

VINOD JOHN (Senior Member, IEEE) received the B.Tech. degree from the Indian Institute of Technology Madras, Chennai, India, in 1992, the M.S.E.E. degree from the University of Minnesota, Minneapolis, MN, USA, in 1994, and the Ph.D. degree from the University of Wisconsin, Madison, WI, USA, in 1999, all in electrical engineering. He is currently a Professor with the Department of Electrical Engineering, Indian Institute of Science, Bangalore, India. His research interests include switched mode power conversion, power quality, and distributed generation.